High spatial resolution measurement of oxygen consumption rates in permeable sediments

Lubos Polerecky[*], Ulrich Franke, Ursula Werner, Björn Grunwald, and Dirk de Beer
Max-Planck Institute for Marine Microbiology, Celsiusstrasse 1, D-28359, Bremen

Abstract

A method is presented for the measurement of depth profiles of volumetric oxygen consumption rates in permeable sediments with high spatial resolution. When combined with in situ oxygen microprofiles measured by microsensors, areal rates of aerobic respiration in sediments can be calculated. The method is useful for characterizing sediments exposed to highly dynamic advective water exchange, such as intertidal sandy sediments. The method is based on percolating the sediment in a sampling core with aerated water and monitoring oxygen in the sediment using either an oxygen microelectrode or a planar oxygen optode. The oxygen consumption rates are determined using three approaches: (1) as the initial rate of oxygen decrease measured at discrete points after the percolation is stopped, (2) from oxygen microprofiles measured sequentially after the percolation is stopped, and (3) as a derivative of steady-state oxygen microprofiles measured during a constant percolation of the sediment. The spatial resolution of a typical 3 to 4 cm profile within a measurement time of 1 to 2 h is better with planar optodes ($\approx$0.3 mm) then with microelectrodes (2 to 5 mm), whereas the precision of oxygen consumption rate measurements at individual points is similar (0.1 to 0.5 μmol L^{-1} min^{-1}) for both sensing methods. The method is consistent with the established methods (interfacial gradients combined with Fick's law of diffusion, benthic-chambers), when tested on the same sediment sample under identical, diffusion-controlled conditions.

Aerobic respiration plays an important role in the degradation of carbon and is typically estimated to account for 25% to 50% of carbon mineralization in coastal sediments. Two established methods have been used for the determination of areal oxygen consumption rates (OCR) in sediments, namely the diffusive oxygen uptake and the benthic-chamber total oxygen uptake methods. The first method, which will be referred to as the flux method, exploits the possibility provided by oxygen microelectrodes to measure diffusive oxygen microprofiles across the sediment-water interface (e.g., Revsbech et al. 1980; Glud et al. 1994). Using Fick's law of diffusion and a measured oxygen microprofile, one can calculate an areal diffusive oxygen uptake rate. However, to obtain an estimation of the possible lateral heterogeneity of areal rates, it is necessary to measure multiple microprofiles, which can be time consuming and requires constant conditions of the system during the measurements. The second method uses a sealed benthic chamber positioned at the surface of the sediment, enclosing a known area of the sediment surface and a known volume of the bottom water (e.g., Pamatmat 1971; Smith 1978; Glud et al. 1994). The areal OCR is evaluated from the temporal decrease of oxygen content in the overlying water in the chamber, which is determined either continuously by, e.g., an oxygen electrode or an oxygen microoptode present in the chamber (Glud et al. 1994; Tengberg et al. 1995; Glud et al. 1996) or by sampling the water from the chamber and analyzing its oxygen content using the Winkler titration technique.

A known problem associated with the flux method is that the obtained areal OCR values can often underestimate the true uptake rates by not including the bio-irrigation activity of macrofauna living in the sediment (for citations, *see* Viollier et al. 2003). This problem is overcome by the benthic-chamber technique, where the measured decrease of oxygen reflects the respiratory activity of all organisms living in the sediment, including bio-irrigating macrofauna. However, the use of a benthic chamber may significantly alter the hydrodynamic

conditions to which the measured sediment is exposed. The diffusive uptake of oxygen by the sediment depends considerably on the thickness of the diffusive boundary layer, which depends strongly on hydrodynamic conditions above the sediment surface. The water inside the chamber is therefore stirred so that the hydrodynamic conditions in the chamber resemble the natural situation as closely as possible.

Advection can be a highly effective transport process across the sediment-water interface (Huettel and Gust 1992; Huettel et al. 1996; Precht and Huettel 2003; Precht et al. 2004), particularly in permeable sediments, which are common in coastal environments (Emery 1968; de Haas et al. 2002). Owing to tidal pumping, waves, or the interaction of the water flow with the surface topography (e.g., ripples), the sediments are flushed with oxygen-rich water, thus significantly enhancing rates of carbon mineralization due to aerobic respiration. In advection-driven systems, the state of oxygenation of the sediment is often very dynamic, making the flux method, based on the measurement of steady-state diffusive microprofiles, unsuitable. Efforts have been made to mimic advective water exchange through the sediment-water interface inside benthic chambers. Cylindrical benthic chambers with stirring-induced radial pressure gradients, as a substitute for horizontal pressure gradients, served as model systems (Glud et al. 1996). Chambers with flexible walls were deployed to allow pressure variations driven by waves to propagate into the chambers (Malan and McLachlan 1991). However, these modifications cannot always mimic the highly dynamic conditions in the systems where advection is the dominant process of oxygen transport, thus limiting the use of benthic chambers under such circumstances.

Recently, an adaptation of eddy correlation to mass flow in aquatic systems was reported (Berg et al. 2003). The method is noninvasive and independent of the transfer mechanism of solutes through the sediment-water interface, which makes it suitable for the study of advective systems. Eddy correlation measures area-integrated fluxes of solutes such as oxygen. The footprint of the method is several square meters, which makes it an attractive tool for the assessment of total solute exchange. The measurement, however, cannot provide the functional information nor the small-scale variability of the processes governing the solute uptake.

The dynamics of oxygen supply in advection-driven systems can be assessed by in situ microprofiling using microelectrodes or planar optodes attached to autonomous profilers (Glud et al. 1994, 1999*a*, 2001; Wenzhöfer and Glud 2002). The variability of oxygen penetration can be determined with high temporal (ranging from a couple of seconds with an optode-based to 10 to 30 min with a microelectrode-based in situ profiler) and spatial (in the sub-millimeter range) resolutions. To estimate the rate of aerobic degradation of organic matter in such sediments, a method is needed for the determination of a depth profile of volumetric OCR with a comparably high spatial resolution. Once a depth profile of volumetric OCR is known, it can be integrated over the depth of

oxygen penetration to obtain areal oxygen uptake rates of the sediment. Such a method was recently introduced by de Beer et al. (2005). It is based on percolating the sediment in a sample core with air-saturated water and observing the decrease of oxygen in the sediment after the percolation is stopped.

In this article, four variations of the basic method introduced by de Beer et al. (2005) are described in detail. The first exploits alternating between the on and off periods of water flow through a sediment column and monitoring with a microelectrode the decrease of oxygen at distinct locations. The second procedure employs oxygen microprofiles measured repeatedly during a single flow-off period. In the third variation, planar oxygen optodes are used to monitor oxygen dynamics in the sediment, allowing a time-efficient determination of a two-dimensional map of OCR with a sub-millimeter spatial resolution. The fourth approach is based on the measurement of steady-state O$_2$ microprofiles during steady percolation of the sediment. Each of the method variations was tried using cores of permeable sandy sediment and compared with the flux and benthic-chamber methods under rigorously controlled conditions. Furthermore, the applicability and limitations of the method are critically assessed and discussed.

Materials and procedures

Materials—The method was applied to permeable sandy sediments collected from an intertidal sandflat in the Wadden Sea (Janssand, near Neuharlingersiel, Germany). The sediment was collected from areas where flushing with oxygen-rich water was, caused by waves and tidal pumping, intense and dynamic (the field data obtained by an autonomous microsensor profiler will be published elsewhere). The porosity of the sediment was $\phi = 0.45$, and the measurements were conducted using seawater (salinity 30) from the study site that was saturated with air at a temperature of 12°C (oxygen concentration 280 µmol L^{-1}).

The flow-through method is assembled schematically as shown in Fig. 1. A core with the sediment sample collected from an area of investigation is first fixed onto a stand so as to allow a flow of water through the sediment in the downward direction. Two types of sediment cores were used for the demonstration of the method reported here: a cylindrical Plexiglas core (inner diameter 36 mm, height 200 mm, wall thickness 3 mm) and a rectangular stainless steel core (inner dimensions 70×75 mm, height 250 mm, wall thickness 2 mm). The Plexiglas core was equipped with a rubber stopper into which a valve was incorporated. The removable bottom of the steel core, also equipped with a valve, contained a depression (3 mm wide, 1 mm deep) with the dimensions fitting the dimensions of the core. The depression was filled with silicone, which enabled watertight enclosure immediately after the collection of the sediment sample.

One side of the steel core contained a polycarbonate window (dimensions $50 \times 150 \times 4$ mm) glued to the steel by silicone. A semi-transparent planar oxygen optode was glued onto the polycarbonate plate by silicone grease (Elastosil, E4,
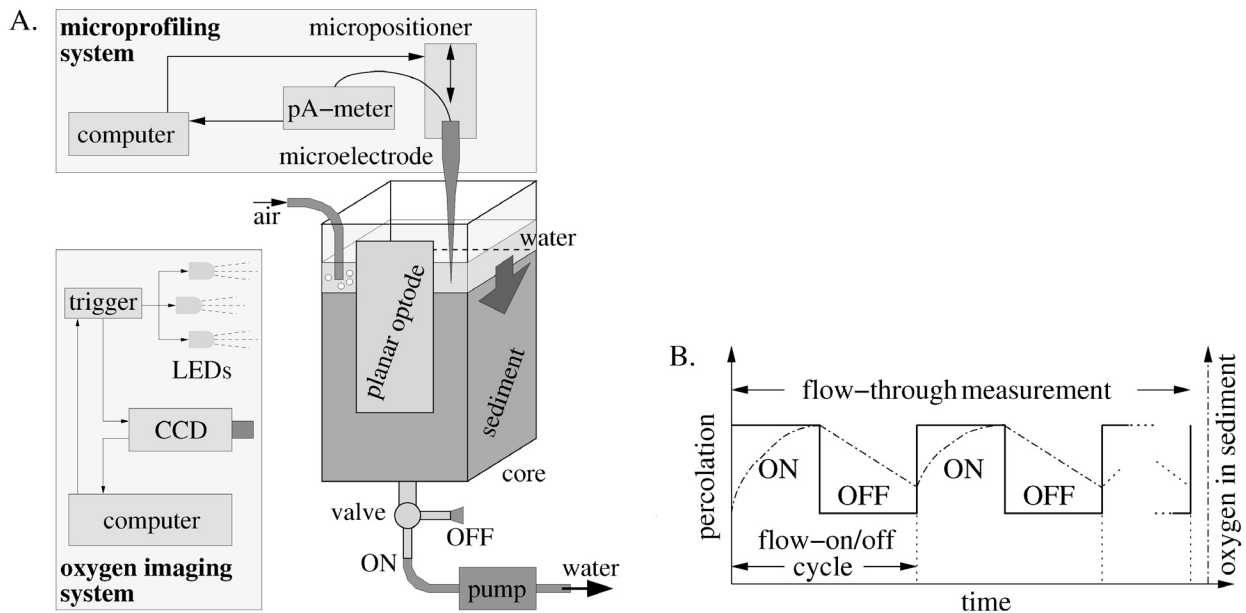
Fig. 1. Schematic diagram of the (A) experimental configuration and (B) timing protocol of the flow-through method.

Wacker) and the firm and water-resistant attachment was reinforced with tape at the foil edges. The foil was inside the core, enabling the measurement of oxygen in the water and sediment in direct contact with the wall. Details of the employed planar optode are given elsewhere (Precht et al. 2004).

The optode measurements were carried out using the MOLLI system (Holst et al. 1998; Holst and Grunwald 2001). The system consisted of a fast gateable charge-coupled device (CCD) camera (SensiCam; PCO), a self-made triggering device, an array of blue light-emitting diodes (LEDs) (LXHL-LB5C, λ_{max} = 470 nm; Lumileds Lighting) with a power supply and a red filter (Amber red; Lee Filters). The measuring software enabled computer-controlled acquisition of images with high spatial resolution and desired timing protocol. Oxygen images were calculated using the rapid lifetime determination method in combination with Stern-Volmer equation describing lifetime quenching by oxygen (Holst et al. 1998).

High spatial resolution oxygen microprofiles were measured with an oxygen microelectrode (Revsbech 1989), which was attached to a micromanipulator placed above the core. The micromanipulator was fixed onto a motorized stage (VT-80; Micos), enabling reproducible positioning of the sensor tip with 1 μm precision. The microelectrode was connected to a high-precision picoammeter, and the meter output was collected by a data-acquisition card (AI-16XE-50, data box CB68-LP; National Instruments). The microprofiling was facilitated by a computer program.

During the measurements, a constant water level above the sediment surface was maintained by a pump regulated by a float lever connected to an electrical switch. The overlying water was kept air-saturated by continuous bubbling with air.

When the permeability of the studied sediment permitted the flow of water solely due to gravity, a valve was used to regulate the speed of water percolation. When the sediment was less permeable, the valve was opened fully and a pump was used to suck the water through the sediment.

Basic theory—Each measurement of OCR consisted of two stages. In the first stage, referred to as the "flow-on" period, the sediment was percolated with air-saturated water. Subsequently, the percolation was stopped (this period is referred to as the "flow-off" period), and the decrease of oxygen in the sediment was recorded (Fig. 1B).

According to the diffusion equation, the rate of decrease of oxygen in the sediment during the flow-off period is determined by (1) the local oxygen consumption rate, denoted as R, and (2) the local concentration variations, mathematically expressed by the diffusion term $D_s \Delta c$, where Δ denotes the Laplacian operator, and D_s is the diffusion coefficient of oxygen in the sediment (Crank 1975). The percolation speed and the duration of the flow-on period of the measurement are selected so that a steady and approximately homogeneous distribution of oxygen is reached in the sediment. This is an important experimental condition, as it guarantees that the diffusive term $D_s \Delta c$ is zero or negligible in comparison with the local consumption rate R at the time when the flow-off period starts. If R is distributed inhomogeneously, local concentration gradients will develop, leading to the measured decrease of oxygen being influenced by the diffusion. Therefore, the local OCR was evaluated as the initial slope of the measured decrease of oxygen concentration.

An alternative approach for determining the depth profile of OCR is based on the theoretical description of the oxygen trans-

port in permeable sediments driven mainly by advection. Under steady flow during the flow-on period, oxygen dissolved in the percolating water is respired on the way through the sediment. In a region of thickness Δz located at depth z of the sediment, the balance of the dissolved oxygen concentration, c, can be written as

$$v_f c(z + \Delta z) - v_f c(z) = - \phi A \Delta z R(z) \tag{1}$$

where v_f is the flow rate in $m^3\,s^{-1}$, $R(z)$ is the local OCR (note that R > 0 refers to oxygen consumption, whereas R < 0 would represent oxygen production) in $mol\,m^{-3}\,s^{-1}$, ϕ is the porosity, and A is the area of the horizontal cross-section in m^2. This equation formulates that the amount of oxygen being transported by water flow at depth $z + \Delta z$ is reduced in comparison to that transported at depth z by an amount consumed in the volume $\Delta V = \phi A \Delta z$ with the consumption rate $R(z)$, which is assumed to be constant in the depth interval between z and $z + \Delta z$.

Considering that the depth difference, Δz, is infinitesimal and v_f is constant with depth, Eq. 1 can be rewritten in the form of a differential equation

$$-\frac{v_f}{\phi A} \frac{\partial c(z)}{\partial z} = R(z) \tag{2}$$

which is a one-dimensional equation describing the variation of an oxygen concentration profile in the sediment in a stationary situation, i.e., $\partial c(z)/\partial t = 0$, where constant advection is the dominant transport mechanism, i.e., $D_s \partial c/\partial z << v_f\, c(z)\,/\,A$. From this equation, it follows that the depth profile of OCR can be determined from the derivative of a stationary oxygen profile during the flow-on period.

Measurement procedure—The measurement of the OCR profile was realized by four different approaches.

1. $O_2(t)$ measured at discrete depths by microelectrode. An oxygen microelectrode was positioned at a specific depth in the sediment and the decrease of oxygen during the flow-off period was recorded. The duration of this period depended on the local oxygen consumption activity of the sediment, and was dynamically selected so that the observed decrease of oxygen was sufficient for precise determination of the slope (typically a couple of minutes). The local OCR was determined as an initial slope of the observed oxygen decrease, obtained by regression analysis. The microelectrode was then repositioned, and the procedure was repeated until a complete OCR profile was measured.

2. Continuous O_2 profiling by microelectrode. Oxygen microprofiles were measured continuously by a microelectrode during the flow-off period (Epping et al. 1999). The OCR profile was determined by subtracting oxygen concentrations measured at different times at individual depths and dividing each value of $\Delta c(z)$ by the time interval between the subsequent oxygen readings. This subtraction was carried out only for nonzero oxygen readings.

3. Continuous O_2 imaging by planar optode. Continuous oxygen imaging was facilitated by the MOLLI system. During the flow-off period, oxygen images were recorded until a significant decrease of oxygen was observed in each pixel (typically for a couple of minutes up to an hour, if the consumption was very slow). The local OCR was determined by evaluating the initial slope of the oxygen decrease in each pixel, resulting in a two-dimensional (2D) map of OCR (*see* text after the following paragraph).

4. O_2 profiling by microelectrode during steady-state flow-on period. Oxygen microprofiles were measured during the flow-on period at different lateral positions. The depth profile of OCR was calculated from the steady state oxygen profiles using Eq. 2, and the known values of the flow speed, porosity, and the cross-section of the sediment core.

Oxygen images were usually superposed with noise, which, depending on the optodes used, was up to ±5% of air saturation. The noise originated from the acquisition of fluorescence images by the CCD camera used and the way the oxygen images were calculated from the raw data (Holst and Grunwald 2001). Such noise levels introduced a complication when determining the initial slope of the oxygen decrease. In particular, when the oxygen images were recorded over sufficient time to ensure that the decrease in oxygen was greater than the noise level in all pixels, the observed oxygen dynamics could be already influenced by the diffusion in some pixels while it was still unaltered in others. This was manifested by the increase or decrease of the observed slope of the oxygen signal in the "diffusion-affected" pixels (depending on whether the pixel is surrounded by a region of a higher or lower consumption activity, respectively), while the linear decrease of oxygen remained unaltered in the diffusion-unaffected pixels.

To distinguish between these types of behavior with a statistical measure of significance, the following strategy was implemented in the pixel-wise determination of the initial slope. The time evolution of oxygen in a pixel i of the image, denoted as $O_2(i;t)$, was fitted with polynomials between the zero and fourth orders, i.e., $O_2(i;t) \doteq P_0(i;t)$, or $O_2(i;t) \doteq P_1(i;t)$, . . . , or $O_2(i;t) \doteq P_4(i;t)$, where $P_k(t) = a_0 + a_1 t + \cdots + a_k t^k$ and each coefficient $a_k \equiv a_k(i)$ is a function of the pixel position. The parameters of the fitting polynomial were obtained by the procedure of minimizing the sum of residues (Kleinbaum and Kupper 1978), i.e., by minimizing the function $\chi_k^2(i) = \Sigma_{n=1}^{N}[O_2(i;t_n) - P_k(i;t_n)]^2$, N being the number of oxygen images considered in the fitting procedure.

The higher the order of the fitting polynomial, the better the quality of the fit, i.e., $\chi_0^2 \geq \chi_1^2 \geq . . . \geq \chi_4^2$. However, even though the fit with a higher order polynomial is better than that with the lower order polynomial, it may not be significantly better. This consideration of a significant improvement of the fit was used to decide by which polynomial the observed evolution $O_2(i;t)$ was eventually fitted. The order of the fitting polynomial was selected as the maximum order K, such that the fit by a polynomial of any higher order, i.e., P_{K+1}, . . . , $P_{k=4,}$ was not significantly better than the fit by the polynomial P_K. The significant improvement was determined by a statistical hypothesis
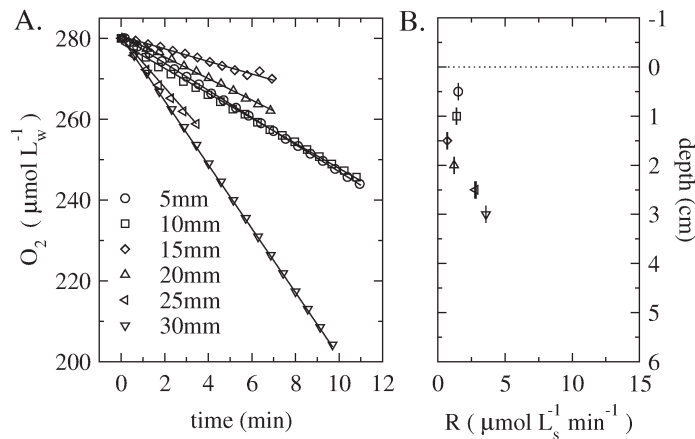
Fig. 2. (A) Time evolution of the oxygen concentration measured at different sediment depths during the flow-off period of the flow-through experiment. (B) Corresponding oxygen consumption rates calculated as the initial slope of the oxygen decrease, corrected for the sediment porosity. The subscripts w and s refer to the volume of porewater and sediment, respectively.

Fig. 3. (A) Oxygen profiles measured during the flow-on (line nr 1) and flow-off (lines nr 2 to 6) periods of the flow-through measurement. Time differences between the starting points of profiles 2 to 3, 3 to 4, 4 to 5, and 5 to 6 were 17, 14, 30, and 34 min, respectively. (B) Corresponding profiles of oxygen consumption rates. Different symbols correspond to different profile pairs. The subscripts w and s refer to the volume of water and sediment, respectively.

testing described in textbooks (Sokal and Rohlf 1995), using the statistical significance level of 0.95. The OCR in the pixel i was then taken as the initial slope of the fitting polynomial (we refer to it as the most suitable polynomial), i.e., equal to the coefficient $a_1(i)$ when $K \geq 1$ or to zero when $K = 0$. This procedure was implemented in a program written in Matlab, enabling the calculation of an OCR image within seconds.

Assessment

$O_2(t)$ measured at discrete depths by microelectrode—The speed of the air-saturated water flow through the sediment was adjusted by the valve to $v_f = 33$ cm^3 min^{-1} and the sediment was percolated for 10 min. The flow-off periods were between 4 and 11 min long, and the corresponding time evolutions of oxygen were recorded at six depths between 5 and 30 mm (Fig. 2A).

The linear decrease of oxygen at each measured depth suggested that the measurements were not influenced by diffusion during the measuring time. The values of OCR, determined from the slope of O_2 $(i;t)$ and shown in Fig. 2B, were expressed per unit of the sediment volume.

One pump-on/off cycle lasted between approximately 15 and 20 min, resulting in the total time necessary to determine a single OCR profile of just under 2 h. The precision of the determined OCR values, taken as the standard error of the slope of the measured $O_2(t)$ at each position, was 0.01 to 0.1 μmol L_s^{-1} min^{-1}. Multiple flow-on/off cycles performed at each position showed that the measurements were reproducible with the same or lower variability. The spatial resolution was rather coarse (5 mm), and the profile was measured only at a single horizontal location (due to time constrains). A statistically representative determination of high resolution depth profiles of OCR would take several days to complete by this
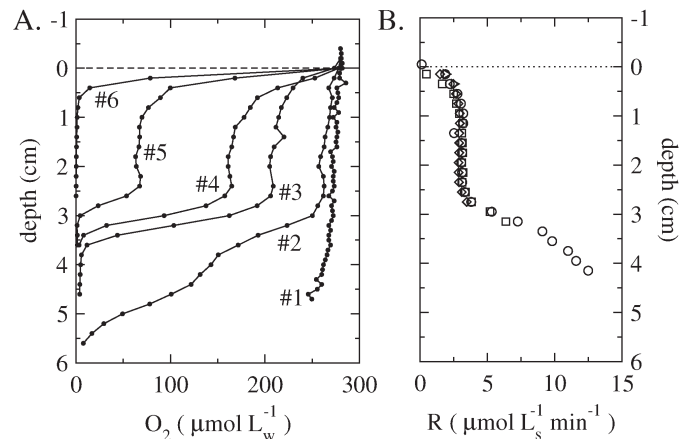
approach, unless multiple sensors are used simultaneously.

Continuous O_2 profiling by microelectrode—The approach based on continuous O_2 profiling by a microelectrode during the flow-off period was repeated on the same sediment core, however, at another horizontal position. Line nr 1 in Fig. 3A shows that initially, during the flow-on period (flow rate $v_f = 33$ cm^3 min^{-1}), oxygen was almost homogeneously distributed in the sediment. During the subsequent flow-off period, oxygen microprofiles were measured in time intervals of 15 to 30 min with a step-size of 2 mm (line nrs 2 to 6 in Fig. 3A).

The procedure described above resulted in OCR profiles shown in Fig. 3B. The OCR profiles obtained by the subtraction of different pairs of microprofiles were almost identical. The same procedure was conducted at another horizontal location, with similar results (data not shown).

The measured OCR profile is very close to that obtained by the approach employing the measurement of $O_2(t)$ at discrete depths, while the spatial resolution was improved (2 mm). However, since the sediment could be profiled, at best, every $\approx$15 min, the individual OCR determinations may include diffusion artifacts. For example, Fig. 3B shows that the measured OCR rapidly increases at depths immediately below 3 cm. This means that local concentration gradients developed during the measurement, leading to a possibly overestimated value of the measured OCR. A similar artifact may be observed near the sediment-water interface, where oxygen may be renewed by diffusion from the overlying water, thus resulting in a possibly underestimated value of OCR.

The degree of underestimation or overestimation can be estimated. This is done by approximating the diffusion contribution as $D_s \partial^2 c / \partial z^2 \approx D_s [c(z + \Delta z) + c(z - \Delta z) - 2c(z)] / \Delta z^2$, where $c(z)$
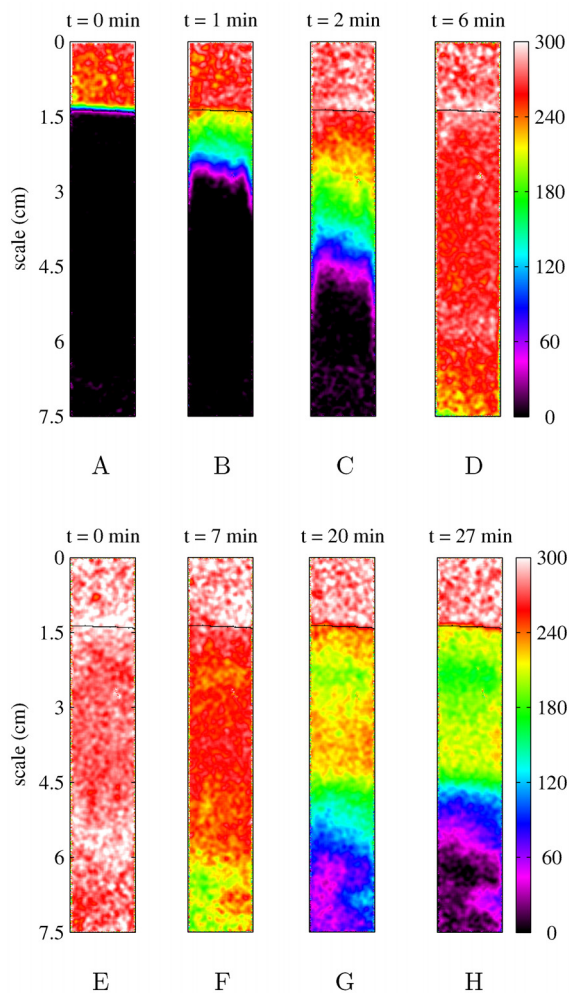
Fig. 4. Examples of oxygen images during the flow-on (A-D) and flow-off (E-H) periods of the flow-through experiment. The solid lines at approximately 1.5 cm indicate the sediment surface. The color-bar on the right indicates the gradation of oxygen concentrations in μmol L_w^{-1}.

Fig. 5. Examples of time evolutions of oxygen in three selected pixels as measured by the planar oxygen optode during the flow-on and flow-off periods. Data denoted as nrs 1, 2, and 3 correspond to selected points located at depths of 1, 3, and 5 cm of the sediment, respectively. Symbols represent the experimental data, solid lines in the bottom graph the most suitable fitting polynomial (*see* text for more details), and dashed lines indicate the initial slope of oxygen decrease, representing the local OCR. For data 1, the dashed line is identical with the fitting line.

is the measured concentration profile and Δz is a depth interval. Using the values from the concentration profile nr 2 around $z = 3$ cm, $\Delta z = 0.4$ cm, and the diffusion coefficient in the sediment of porosity $\phi = 0.45$ of $D_s = 0.9 \times 10^{-5}$ cm^2 s^{-1} (Boudreau 1996), the diffusive term amounts to ≈ -0.17 μmol L_s^{-1} min^{-1}. Using the values from profile nr 5 around $z = 0.5$ cm and the same D_s and Δz, the diffusive term amounts to ≈ 0.54 μmol L_s^{-1} min^{-1}. Consequently, a conservative estimation of the inaccuracy of the measured OCR ranges between approximately -0.2 and 0.6 μmol L_s^{-1} min^{-1} for the deeper parts of the sediment ($z \geq 3$ cm) and for the locations close to the sediment-water interface ($z \leq 0.5$ cm), respectively. Thus the error induced by diffusion is less than 10%.

Since the OCR values obtained from different pairs of the measured oxygen profiles were similar, the OCR profile can be satisfactorily determined by measuring only two sequential profiles during the flow-off period. Thus, a depth profile of OCR between 0 and 4 cm with a spatial resolution of 2 mm could be
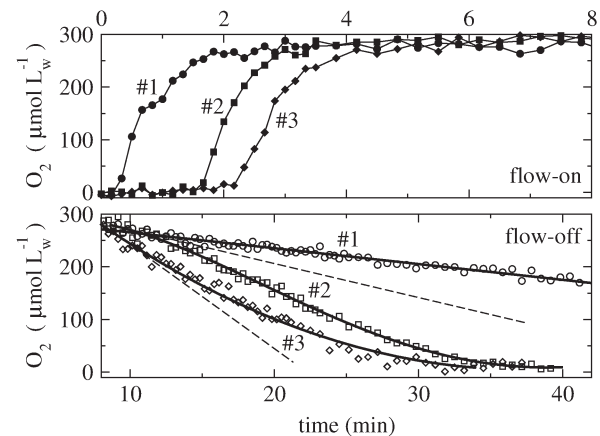
determined with a needle-type microsensor within 30 to 60 min.

Continuous O$_2$ imaging by planar optode—The sediment sample was collected from the same site using a steel core with a window containing a planar oxygen optode. Approximately 2/3 of the optode was covered by the sediment and the remaining 1/3 by the overlying water.

The CCD camera was positioned so that the area of the planar optode (25 × 150 mm) resulted in an oxygen image of size 80 × 480 pixels, implying a spatial resolution of ≈300 μm. To minimize the noise of the oxygen images, 4 and 8 sequential images were averaged, resulting in a temporal resolution of ≈5 and 10 s during the flow-on and flow-off periods, respectively.

Penetration of oxygen into the sediment during the flow-on period was observed in real time (*see* Fig. 4A to 4D). At a flow speed of 50 cm^3 min^{-1}, an approximately homogeneous distribution of oxygen in the sediment was reached after 8 min. Examples of the images recorded during the flow-off period, which lasted for 40 min, are shown in Fig. 4E to 4H. To check for the reproducibility of the measurement, the same procedure was repeated two more times.

Typical examples of time evolutions of the oxygen concentration in three selected pixels of the oxygen images are shown in Fig. 5. The pixels were selected to demonstrate different types of oxygen dynamics in the sediment. The data denoted as nr 1 in the bottom graph depict the decrease of oxygen concentration unaltered by diffusion during the entire duration of the flow-off period. On the other hand, the data denoted as nr 2 and 3 demonstrate how diffusion can increase and decrease the initial rate of oxygen consumption, respectively.

Figure 5 also shows the results of the fitting procedure. For example, the order of the most suitable polynomial fitting the
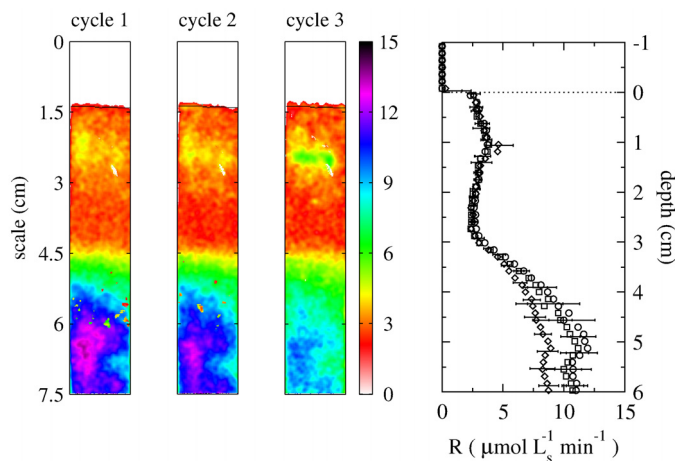
Fig. 6. Examples of OCR images obtained from three subsequent flow-through cycles. The color bar to the right of the OCR images indicates the correspondence between the color and OCR in μmol L_s^{-1} min^{-1}. Depth profiles of OCR, obtained by horizontal averaging of the images, are also shown (circles, squares, and diamonds correspond to the cycles 1, 2, and 3, respectively). The error bars represent the horizontal variability of the sediment's OCR. For clarity, only every fifth vertical data-point is depicted, i.e., every 1.5 mm.

Fig. 7. (A) Stationary oxygen profiles measured during the flow-on period at various horizontal positions. (B) Depth profile (symbols) of OCR obtained as the average of the OCR depth profiles calculated from Eq. 2 and the stationary profiles in A. The corresponding rate of water filtration through the sediment as a function of oxygen penetration depth z_p is depicted by a solid line.

data nr 1, nr 2, and nr 3 was 1, 3, and 2, respectively. The corresponding initial slopes, representing the local OCR, are depicted by the dashed lines. In addition to the local OCR, the fitting procedure also revealed the standard deviation of the initial slope, namely 0.05, 0.5, and 0.25 μmol L_s^{-1} min^{-1} for data nr 1, nr 2, and nr 3, respectively. Thus the precision of the OCR values in a randomly selected pixel can be conservatively estimated as $\approx \pm 0.5$ μmol L_s^{-1} min^{-1}.

After the fitting procedure was carried out in every pixel of the oxygen images, 2D maps of OCR across the entire observed section of the sediment were obtained (Fig. 6). After averaging the images in the horizontal direction, depth profiles of OCR were obtained, as shown in the same figure. The error bars, obtained as the standard deviations of the OCR values at the corresponding horizontal section, indicate the variability of sediment oxygen consumption over small horizontal scales.

The profiles obtained by planar optodes agree well with the profiles determined by the microelectrode-based approaches (compare Fig. 6 with Figs. 2 and 3). This demonstrates a consistency of the measurement approaches. The planar optode–based approach, however, provides a number of benefits.

First, planar optodes enable the acquisition of a large amount of information during a single flow-on/off cycle of the flow-through measurement (Fig. 1B). In particular, the spatial resolution is optimal (≈ 300 μm, as compared to 2 to 5 mm achieved by a microelectrode in approximately the same measuring time), and both the vertical and horizontal small-scale variability of oxygen consumption activity of the sediment can be assessed. Second, since the planar optodes enable the observation of the oxygen distributions in real time, the timing of the flow-through measurement can be
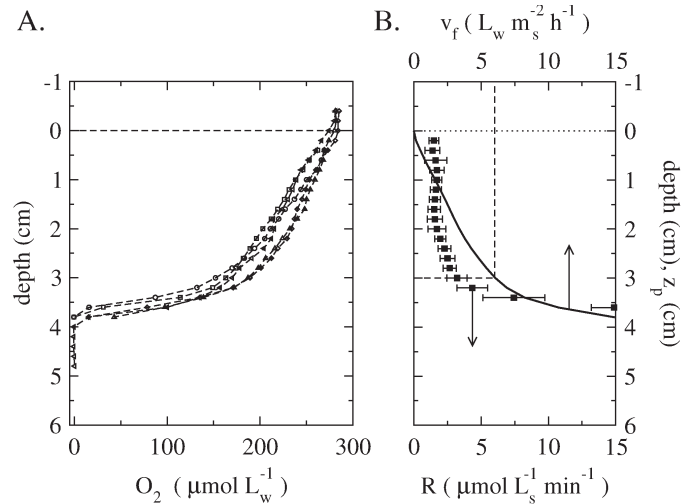
optimized dynamically.

A drawback of planar optodes is that the signal-to-noise ratio is lower than that of microelectrodes. This may lead to less precise OCR values (in the order of $\approx \pm 0.5$ μmol L_s^{-1} min^{-1}, as mentioned above).

When using a microelectrode, OCR can be determined at any point in the sediment, which is an advantage in comparison to the planar optode–based approach, where the measurement is restricted to the region of the sediment in direct contact with the optode. The OCR obtained by microelectrodes and planar optodes are similar, thus wall effects may be assumed to have been insignificant during this method demonstration.

Another potential drawback related to measurement with optodes is that the determination of oxygen requires intensive blue excitation light. If the sediment contains phototactic microorganisms, the OCR could be altered if light exposure is long enough to allow for migration of such organisms toward the wall. Also, if photosynthetic microorganisms were present in the sediment, oxygen production induced by the measuring light could influence the OCR measurement. However, such problems could be avoided by the use of optically isolated planar optodes (Glud et al. 1998, 1999*b*).

O_2 profiling during steady-state flow-on period—The flow-through method employing O_2 profiling by a microelectrode during the steady-state flow-on period was tested using the same sediment core characterized with the other microelectrode-based approaches. The water flow was, however, significantly lowered to $v_f = 0.25$ cm^3 min^{-1}, which corresponded to a porewater flow velocity of 3.3 cm h^{-1}. During the flow-on period, oxygen profiles were determined by a microelectrode

at different horizontal positions. After approximately 2 h, stationary oxygen profiles were measured, as shown in Fig. 7A. Each profile was fitted by a model describing advective transport of oxygen in the sediment (Eq. 2), leading to a depth profile of OCR. These depth profiles were averaged, and the resulting mean values together with the standard deviations are shown by symbols in Fig. 7B.

The OCR values agree very well with those obtained by the alternative microelectrode-based methods described above. The effect of diffusion, given by the second derivative of the profile multiplied by the diffusion coefficient, was also evaluated, but no significant influence on the OCR values was found.

Results obtained under steady flow can also be viewed as mimicking in situ oxygen profiles. An important parameter obtained by autonomous in situ profilers is the dynamic penetration depth of oxygen. The question is whether the volumetric exchange rate of water through the sediment could be estimated from this parameter.

Although natural flows are usually more complex (*see* below), the advective transport of porewater through many permeable sediments can be thought of as similar to that during the flow-on period of the flow-through measurements. During the measurement described above, the oxygen penetration depth of ≈ 3.7 cm was achieved with the porewater flow of 3.3 cm h^{-1}, or the overlying water flow of 1.5 cm h^{-1} = 15 L m^{-2} h^{-1} (*see* the oxygen profiles in Fig. 7A). Thus, if such a penetration depth was observed by in situ microprofiling, it could be estimated that approximately 15 L of overlying water is filtered hourly through every m^2 of the sediment.

If another oxygen penetration depth was measured, additional "mimicking" measurements would not be necessary. Since the depth profile of OCR was already measured, advection-governed oxygen profile and thus the penetration depth can be modeled from Eq. 2. Denoting the oxygen concentration in the overlying water by c_0, penetration depth of oxygen by z_p, and assuming that the values of the porewater flow and porosity do not vary with depth, integration of Eq. 2 leads to $c_0 v_f / \phi A = \int_0^{z_p} R(z) dz$. Using this equation, which is nothing but a simple oxygen balance for a steady-state vertical water flow, v_f can be estimated from the measured z_p and OCR profile $R(z)$, or vice versa.

The possible shape of $v_f(z_p)$ was calculated from the measured OCR profile and is shown by a solid line in Fig. 7B. When OCR is approximately constant (depths between 0 and 3 cm), the oxygen penetration depth increases roughly linearly with the flow rate. At 6 L_w m$_s^{-2}$ h^{-1}, it reaches 3 cm, i.e., approximately 6 L of overlying water is filtered hourly through every m^2 of sediment when oxygen penetrates 3 cm deep. OCR rapidly increases below 3 cm and, consequently, the oxygen penetration depth is much less sensitive to the flow rate. For example, even though v_f doubles from ≈ 7.5 L_w m$_s^{-2}$ h^{-1} to ≈ 15 L_w m$_s^{-2}$ h^{-1}, the penetration of oxygen increases only by as little as 5 mm (from ≈ 3.3 to ≈ 3.8 cm).

These observations suggest that in situ filtration rates of the sediment (porewater flow rates) could be estimated from OCR

profiles when in situ oxygen penetration depths are also measured. This could be an interesting and attractive application of the flow-through method, since in situ filtration rates in permeable sediments have only been determined thus far by elaborate measurements of the displacement of an indicator (e.g., fluorescent dye or iodide) injected into the sediment (Precht and Huettel 2004; Reimers et al. 2004). One should, however, bear in mind the difference between the simple down-flow implemented in the flow-through method and the more complex water exchange in natural sediments (*see* Shum 1992; Shum and Sundby 1996; Huettel et al. 1996; Precht et al. 2004 for more on this topic).

The patterns of oxygen distributions resulting from the complex water exchange in permeable sediments can be determined in two dimensions (Precht et al. 2004; Wenzhöfer and Glud 2004). Provided that the directional field of the porewater flow is known, or can be, to some extent, reliably estimated, the model of advective transport expanded to two dimensions can be used together with the two-dimensional oxygen images to quantify the flow rate. Specifically, the process would involve (1) the calculation of the spatial derivative of concentration along the direction of the porewater flow vector, i.e., $\Delta_{\vec{s}} c$, where $\vec{s} \parallel \vec{v}_f$, and (2) the calculation of the time derivative of concentration, $\partial c / \partial t$, determined from oxygen images acquired at different times. Consequently, neglecting the diffusive transport, the magnitude of the local flow rate (in cm h^{-1}) could be estimated from $v_f / \phi A \approx (\partial c / \partial t - R) \mid \nabla_{\vec{s}} c \mid^{-1}$, where R is the two-dimensional OCR distribution determined by the planar optode–based flow-through method. The pursuit of such an interesting application would, however, require further investigation beyond the scope of this article.

Comparison of the flow-through method with the flux and benthic-chamber methods—The flow-through method was compared with the commonly used techniques for the determination of the areal oxygen consumption rates, i.e., the flux and benthic-chamber methods, under diffusion-dominated conditions. The purpose of this test was to confirm the consistency among the methods under well controlled conditions, where all methods are directly applicable.

The core with the planar optode was filled with sieved sediment of porosity $\phi = 0.45$. The water above the sediment was kept air saturated and stirred with a small propeller attached to a rotating axis. Stirring was minimal to ensure that transport was entirely diffusive.

Firstly, multiple microprofiles were measured by an oxygen microelectrode at different horizontal positions across the sediment surface area. The concentrations, which decreased by 23 ± 3 μmol L^{-1} over the average diffusive boundary layer thickness of 500 μm (measured profiles not shown), were fitted by a diffusive model. Using the diffusion coefficient $D_w = 2 \times 10^{-5}$ cm^2 s^{-1}, the average oxygen flux at the sediment-water interface was $J_{flux} = 5.4 \pm 0.9$ μmol m^{-2} min^{-1}.

The second step consisted of a planar optode–based flow-through measurement with the flow-on period lasting approxi-

mately 2 min. At each horizontal position of the calculated OCR image, the vertical OCR profile was integrated over the penetration depth of oxygen ($\approx$5 mm). The penetration depth was determined sufficiently long before and after the flow-through measurement, i.e., when oxygen distribution was governed by diffusion. This way the obtained values could directly be compared with those from the first and next steps (*see* the following paragraph). The resulting rates were averaged, leading to a total areal oxygen uptake rate of $J_{flow\text{-}through}$ = 5.0 ± 1.0 µmol m^{-2} min^{-1}.

Finally, a measurement mimicking the benthic-chamber experiment was carried out. Aeration of the overlying water was stopped and the chamber was closed with a lid. Stirring of the overlying water continued to maintain the same thickness of the diffusive boundary layer as during the diffusive flux measurement. The decrease of oxygen in the overlying water was monitored by an oxygen microelectrode positioned 1 cm above the sediment surface as well as by the planar optode, which extended well above the sediment surface. From the decrease, determined by regression analysis, the volume of the overlying water and the area of the sediment surface, the oxygen uptake rate was found to be $J_{chamber}$ = 5.3 ± 0.1 µmol m^{-2} min^{-1}.

The obtained values confirm that the three techniques lead to consistent results, when tested under equivalent, well-controlled, diffusion-dominated conditions. However, since the flow-through method determines the potential volumetric OCR independently of the oxygenation status of the sediment, its applicability is much broader than that of the flux or benthic-chamber methods (*see* Discussion for more on this topic).

It should be noticed that the standard deviation of the oxygen uptake rate obtained by the benthic-chamber method was approximately 9 to 10 times smaller than that obtained by the other two methods. This is understandable, as the standard deviations evaluated for the flux and flow-through methods represent the small-scale horizontal variability of the sediment with regard to the oxygen uptake rates, which is averaged by the benthic-chamber technique.

Effects of water percolation on the measurement—To identify potential artifacts induced by the percolation of air-saturated water through the sediment, results obtained by the planar optode–based approach were further analyzed. The OCR images and the corresponding depth profiles of OCR displayed in Fig. 6 demonstrate that the OCR measured in cycle $N + 1$ were lower than those measured in cycle N in nearly all pixels. This was a consistently observed effect when the cycles were measured immediately one after the other. On the other hand, if the gap between the cycles was much longer, e.g., overnight, a recovery in the measured OCR to the original values was observed (data not shown). The effect was much more pronounced in deeper parts of the sediment (below 3 cm in the example discussed here), which coincided with a distinctly differently colored sediment (dark gray, almost black), as opposed to a light-brown sediment of the top 3 cm.

This effect is most likely due to sediment stratification developed under natural conditions as a result of a highly dynamic, advection-driven supply of oxygen into the sediment induced by waves and tidal pumping. Oxygen penetration depths of 2 to 3 cm are frequently observed by in situ profiler measurements (Walpersdorf unpubl. data unref.), suggesting that the top sediment layer is inhabited mainly by aerobically respiring organisms, whereas reduced compounds accumulated in the deeper sediment. During the flow-through measurement, the pool of reduced compounds that can be easily oxidized contributed to the observed OCR in the deeper part of the sediment. As a result of this chemical oxidation, the size of the pool was reduced, resulting in the decreased contribution to the OCR observed in the subsequent measurement. On the other hand, when the sediment was kept anoxic for a longer time period, the pool could recover, resulting in a higher observed OCR.

Percolation of the sediment sample with aerated water is a prerequisite for the method, leading to a possible flushing out of compounds dissolved in the porewater from the sediment. Furthermore, rather lengthy percolation periods are required when a microelectrode-based approach is employed. This may lead to a possible underestimation of the real oxygen consumption activity, as discussed above. However, as shown in Fig. 6, these effects are not significant in the part of the sediment that is naturally exposed to oxic conditions, which is the zone of primary interest.

Reimers et al. (2004) recently reported that the areal consumption rate of the same sediment volume could be enhanced by an increased percolation rate. Greater dispersion and penetration of oxygenated water into anoxic microenvironments within heterogeneous sediment at higher flow rates was suggested as a possible cause of this effect. Our measurements support this view, although additional experiments would be needed to exclude the possibility that respiration activities of microorganisms are enhanced by higher porewater flow rates. Using planar optodes, it was possible to monitor in real time the distribution of oxygen in the sediment. When OCR at some regions (not necessarily microscopic) of the sediment exceeded the supply of oxygen by the percolation at a specific flow rate, the regions remained anoxic. This would result in effectively zero potential volumetric OCR in these regions, leading after integration to lower areal OCR. If the flow rate was increased until the entire sediment in front of the optode was oxic, the subsequently calculated OCR image showed significantly higher rates at these regions. Therefore, when sufficiently high percolation rates are used, the flow-through method provides an estimate of the maximum areal OCR. The percolation could, however, be modified to reflect the porewater flow conditions observed in situ (if such data exist), thus providing an estimate of the total oxygen uptake by the sediment experiencing close to natural conditions.

Comments and recommendations

The flow-through method is, in principle, a laboratory technique and cannot easily be applied in situ. However, since the experimental setup can be relatively easily assembled, it can

Table 1. Duration, spatial resolution, and precision of the different approaches of the flow-through measurement for a typical 3 to 4 cm vertical OCR profile determined by an oxygen microelectrode (ME) or planar optode (PO)

Measurement approach	Measurement time of one OCR profile	Spatial resolution (mm)	Precision (μmol L^{-1} min^{-1})
O$_2$(t) at discrete depths (ME)	2 h	2 to 5	0.01 to 0.1
Continuous O$_2$ profiling (ME)	30 to 60 min	2	0.5
Continuous O$_2$ imaging (PO)	20 to 30 min	0.3	0.5
O$_2$ profiling during steady flow (ME)	2 to 4 h	2	0.5

be used as a field technique enabling the measurement immediately after the collection of the sample from a studied site.

The measurement procedure is simple, and the software tools providing the subsequent analysis of the results were designed so that they could be operated by a trained nonspecialist. Only minimal instrumentation (a micropositioner, an oxygen microelectrode, and a data acquisition system) is required when the approach based on O$_2$(t) measurements at discrete depths is employed. An additional automated micropositioning setup is preferable if the approaches based on continuous O$_2$ profiling during the flow-on or flow-off periods are used. With the access to a lifetime imaging system and planar oxygen optodes, full benefits of the flow-through method, namely the rapid determination of OCR in 2D with high spatial resolution, can be exploited. It is preferable to conduct planar optode measurements under dark conditions or at least at low ambient light intensities. No special light conditions are required for the microelectrode-based approach, unless potential photosynthesis needs to be avoided. Typical merits characterizing each approach of the flow-through method are summarized in Table 1.

The flow-through method has a distinct advantage over the flux and benthic-chamber methods, as it quantifies the spatial distribution of potential oxygen consumption rates independently of the in situ conditions in the sediment. To determine actual in situ oxygen uptake rates, the results must be combined with information gathered when in situ oxygen distributions are measured in the sediment. It is not necessary to describe or mimic natural levels of flow complexity when quantifying OCR. It is only necessary to know over what depth to integrate the OCR profile.

Due to the reliance of the flow-through method on supplementary information provided by benthic in situ profilers, its application may be costlier in comparison to, e.g., the benthic-chamber method. However, due to the above-mentioned advantage, the flow-through method provides more accurate results in sediments with highly dynamic conditions (flow and oxygen penetration), where the use of benthic-chambers is limited and the flux method is not applicable.

The use of the flow-through method is limited in sediments with abundant burrowing and bioirrigating macrofauna. This is mainly because macrofauna can locally disturb the assessment of the rates by its irregular activity (i.e., water pumping) during the measurement. Another problem is that the respiring macrofauna can be easily missed if microelectrodes are

used or if macrofauna are not located in sections of sediment in contact with planar optodes. Even though the volumetric respiration rates due to macrofauna can be determined, a straightforward quantification of areal OCR of the sediment would be problematic and the benthic-chamber or eddy-correlation technique would provide more reliable results.

The use of planar optodes facilitates a high spatial resolution measurement of OCR in two dimensions. This provides an insight into the sediment and the functional variability of the processes governing the oxygen uptake, e.g., allows to differentiate between the microbial activity and bioturbation or bioirrigation, which is not possible using the benthic-chamber or eddy-correlation techniques.

In conclusion, the proposed method provides a feasible technique for the determination of volumetric oxygen consumption rates with high spatial resolution. The method is most suitable for permeable sediments, which can be easily percolated with water and which are naturally exposed to highly dynamic conditions. Of particular interest are sandy sediments, such as coral sands, intertidal or subtidal lithogenous sands, river beds, and seep sediments.

References

Berg, P., H. Røy, F. Janssen, V. Meyer, B. B. Jørgensen, M. Huettel, and D. de Beer. 2003. Oxygen uptake by aquatic sediments measured with a novel non-invasive eddy-correlation technique. Mar. Ecol. Prog. Ser. 261:75-83.

Boudreau, B. P. 1996. The diffusive tortuosity of fine-grained unlithified sediments. Geochim. Cosmochim. Acta 60(16): 3139-3142.

Crank, J. 1975. Mathematics of diffusion. Oxford University Press, 2nd edition.

de Beer, D., and others. 2005. Transport and mineralization rates in North Sea sandy intertidal sediments (Sylt-Rømø basin, Wadden Sea). Limnol. Oceanogr. 50(1):113-127.

de Haas, H., T. C. E. van Weering, and H. de Stigter. 2002. Organic carbon in shelf seas: sinks or sources, processes and products. Continent. Shelf Res. 22(5):691-717.

Emery, K. O. 1968. Relict sediments on continental shelves of the world. Am. Assoc. Petrol. Geol. 52:445-464.

Epping, E. H. G., A. Khalili, and R. Thar. 1999. Photosynthesis and the dynamics of oxygen consumption in a microbial mat as calculated from transient oxygen microprofiles. Limnol. Oceanogr. 44(8):1936-1948.

Glud, R. N., S. Forster, and M. Huettel. 1996. Influence of radial pressure gradients on solute exchange in stirred benthic chambers. Mar. Ecol. Prog. Ser. 141(1-3):303-311.

———, J. K. Gundersen, B. B. Jørgensen, N. P. Revsbech, and H. D. Schulz. 1994. Diffusive and total oxygen-uptake of deep-sea sediments in the eastern south-Atlantic ocean—in-situ and laboratory measurements. Deep-Sea Res. Part I Oceanogr. Res. Pap. 41(11-12):1767-1788.

———, I. Klimant, G. Holst, O. Kohls, V. Meyer, M. Kühl, and J. K. Gundersen. 1999*a*. Adaptation, test and in situ measurements with O_2 microopt(r)odes on benthic landers. Deep-Sea Res. Part I Oceanogr. Res. Pap. 46(1):171-183.

———, M. Kühl, O. Kohls, and N. B. Ramsing. 1999*b*. Heterogeneity of oxygen production and consumption in a photosynthetic microbial mat as studied by planar optodes. J. Phycol. 35(2):270-279.

———, C. M. Santegoeds, D. De Beer, O. Kohls, and N. B. Ramsing. 1998. Oxygen dynamics at the base of a biofilm studied with planar optodes. Aquat. Microb. Ecol. 14(3):223-233.

———, A. Tengberg, M. Kühl, P. O. J. Hall, I. Klimant, and G. Holst. 2001. An in situ instrument for planar O_2 optode measurements at benthic interfaces. Limnol. Oceanogr. 46(8):2073-2080.

Holst, G., and B. Grunwald. 2001. Luminescence lifetime imaging with transparent oxygen optodes. Sens. Actuators B Chem. 74(1-3):78-90.

———, O. Kohls, I. Klimant, B. Konig, M. Kühl, and T. Richter. 1998. A modular luminescence lifetime imaging system for mapping oxygen distribution in biological samples. Sens. Actuators B Chem. 51(1-3):163-170.

Huettel, M., and G. Gust. 1992. Impact of bioroughness on interfacial solute exchange in permeable sediments. Mar. Ecol. Prog. Ser. 89(2-3):253-267.

———, W. Ziebis, and S. Forster. 1996. Flow-induced uptake of particulate matter in permeable sediments. Limnol. Oceanogr. 41(2):309-322.

Kleinbaum, D. G., and L. L. Kupper. 1978. Applied regression analysis and other multivariable methods. Duxbury Press.

Malan, D. E., and A. McLachlan. 1991. In situ benthic oxygen fluxes in a nearshore coastal marine system: a new approach to quantify the effect of wave action. Mar. Ecol. Prog. Ser. 73:69-81.

Pamatmat, M. M. 1971. Oxygen consumption by the seabed IV. Shipboard and laborator experiments. Limnol. Oceanogr. 16:536-550.

Precht, E., U. Franke, L. Polerecky, and M. Huettel. 2004. Oxygen dynamics in permeable sediments with wave-driven porewater exchange. Limnol. Oceanogr. 49(3):693-705.

——— and M. Huettel. 2003. Advective porewater exchange driven by surface gravity waves and its ecological implications. Limnol. Oceanogr. 48(4):1674-1684.

——— and M. Huettel. 2004. Rapid wave-driven advective porewater exchange in a permeable coastal sediment. J. Sea Res. 51:93-107.

Reimers, C. E., and others. 2004. In situ measurements of advective solute transport in permeable shelf sands. Continent. Shelf Res. 24:183-201.

Revsbech, N. P. 1989. An oxygen microelectrode with a guard cathode. Limnol. Oceanogr. 34(2):474-478.

———, J. Sørensen, T. H. Blackburn, and J. P. Lomholt. 1980. Distribution of oxygen in marine sediments measured with microelectrodes. Limnol. Oceanogr. 25(3):403-411.

Shum, K. T. 1992. Wave-induced advective transport below a rippled water-sediment interface. J. Geophys. Rese. Oceans 97:789-808.

——— and B. Sundby. 1996. Organic matter processing in continental shelf sediments—the subtidal pump revisited. Mar. Chem. 53:81-87.

Smith, K. L. 1978. Benthic community respiration in NW Atlantic Ocean—in situ measurements from 40 to 5200 M. Mar. Biol. 47(4):337-347.

Sokal, R. R., and F. J. Rohlf. 1995. Biometry, 3rd edition. W. H. Freeman and Company.

Tengberg, A., and others. 1995. Benthic chamber and profiling landers in oceanography—A review of design, technical solutions and functioning. Prog. Oceanogr. 35(3):253-294.

Viollier, E., and others. 2003. Benthic biogeochemistry: state of the art technologies and guidelines for the future of in situ survey. J. Exp. Mar. Biol. Ecol. 285-286:5-31.

Wenzhöfer, F., and R. N. Glud. 2002. Benthic carbon mineralization in the Atlantic: a synthesis based on in situ data from the last decade. Deep-Sea Res. I Oceanogr. Res. Pap. 49(7):1255-1279.

——— and R. N. Glud. 2004. Small-scale spatial and temporal variability in coastal benthic O_2 dynamics: Effects of fauna activity. Limnol. Oceanogr. 49:1471-1481.